A Turbo Detection and Sphere-Packing-Modulation-Aided Space-Time Coding Scheme

Osamah Rashed Alamri, Bee Leong Yeap, and Lajos Hanzo, *Fellow, IEEE*

***Abstract*—A recently proposed space-time block-coding (STBC) signal-construction method that combines orthogonal design with sphere packing (SP), referred to here as STBC-SP, has shown useful performance improvements over Alamouti's conventional orthogonal design. In this contribution, we demonstrate that the performance of STBC-SP systems can be further improved by concatenating SP-aided modulation with channel coding and performing demapping as well as channel decoding iteratively. We also investigate the convergence behavior of this concatenated scheme with the aid of extrinsic-information-transfer charts. The proposed turbo-detected STBC-SP scheme exhibits a "turbo-cliff" at $E_b/N_0 = 2.5$ dB and provides E_b/N_0 gains of approximately 20.2 and 2.0 dB at a bit error rate of 10^{-5} over an equivalent-throughput uncoded STBC-SP scheme and a turbo-detected quadrature phase shift keying (QPSK) modulated STBC scheme, respectively, when communicating over a correlated Rayleigh fading channel.[1]**

***Index Terms*—EXIT charts, iterative demapping, multidimensional mapping, space-time coding, sphere packing, turbo detection.**

I. Introduction

THE ADVERSE effects of channel fading may be significantly reduced by employing space-time coding invoking multiple antennas [1]. Alamouti [2] discovered an appealingly simple transmit-diversity scheme employing two transmit antennas. This low-complexity design inspired Tarokh *et al.* [3], [4] to generalize Alamouti's transmit-diversity scheme using the principle of orthogonal design to an arbitrary number of transmit antennas. Since then, the pursuit of designing better space-time modulation schemes has attracted considerable further attention [5]. The concept of combining orthogonal transmit-diversity designs with the principle of sphere packing (SP) was introduced by Su *et al.* in [6]. Orthogonal transmit-diversity designs can be described recursively [7] as follows. Let $\mathbf{G}_1(x_1) = x_1\mathbf{I}_1$, and let

$$\mathbf{G}_{2^k}(x_1,\ldots,x_{k+1}) = \begin{bmatrix} \mathbf{G}_{2^{k-1}}(x_1,\ldots,x_k) & x_{k+1}\mathbf{I}_{2^{k-1}} \\ -x_{k+1}^*\mathbf{I}_{2^{k-1}} & \mathbf{G}^{\mathcal{H}}_{2^{k-1}}(x_1,\ldots,x_k) \end{bmatrix}$$

for $k = 1, 2, 3, \ldots$, where x_{k+1}^* is the complex conjugate of x_{k+1}, $\mathbf{G}^{\mathcal{H}}_{2^{k-1}}(x_1,\ldots,x_k)$ is the Hermitian of $\mathbf{G}_{2^{k-1}}(x_1,\ldots,x_k)$, and $\mathbf{I}_{2^{k-1}}$ is a $(2^{k-1}\times 2^{k-1})$ identity matrix. Then, $\mathbf{G}_{2^k}(x_1,x_2,\ldots,x_{k+1})$ constitutes an orthogonal design of size $(2^k\times 2^k)$, which maps the complex variables representing $(x_1,x_2,\ldots,x_{k+1})$ to 2^k transmit antennas. In other words, $x_1,x_2,\ldots,x_{k+1}$ represent $k+1$ complex modulated symbols to be transmitted from 2^k transmit antennas in $T=2^k$ time slots. It was shown in [6] that the diversity product quantifying coding advantage[2] of an orthogonal transmit-diversity scheme is determined by the minimum Euclidean distance of the vectors $(x_1,x_2,\ldots,x_{k+1})$. Therefore, in order to maximize the achievable coding advantage, it was proposed in [6] to use SP schemes that have the best-known minimum Euclidean distance in the $2(k+1)$-dimensional real-valued Euclidean space $\mathbb{R}^{2(k+1)}$ [8]. The results of [6] demonstrated that the proposed SP-aided space-time block-coded (STBC) system of Section II, referred to here as STBC-SP, was capable of outperforming the conventional orthogonal-design-based STBC schemes of [2] and [3].

Iterative decoding of spectrally efficient modulation schemes was considered by several authors [1], [9]–[11]. In [12], the employment of the turbo principle was considered for iterative soft demapping in the context of multilevel-modulation schemes combined with channel decoding, where a soft demapper was used between the multilevel demodulator and the channel decoder. In [13], a turbo-coding scheme was proposed for the multiple-input–multiple-output (MIMO) Rayleigh fading channel, where an additional block code was employed as an outer channel code, while an orthogonal STBC scheme was considered as the inner code.

Recently, studying the convergence behavior of iterative decoding has attracted considerable attention [14]–[24]. In order to determine the E_b/N_0 convergence threshold of randomly constructed irregular low-density–parity-check (LDPC) codes

Manuscript received April 25, 2005; revised December 22, 2005 and March 19, 2006. This work was supported in part by the EPSRC, U.K., in part by the European Union under the auspices of the Phoenix and Newcom projects, and in part by the Ministry of Higher Education of Saudi Arabia. The review of this paper was coordinated by Dr. M. Reed.

O. R. Alamri and L. Hanzo are with the School of Electronics and Computer Science, University of Southampton, SO17 1BJ Southampton, U.K. (e-mail: ora02r@ecs.soton.ac.uk; lh@ecs.soton.ac.uk).

B. L. Yeap was with the School of Electronics and Computer Science, University of Southampton, SO17 1BJ Southampton, U.K. He is now with Radioscape, NW1 4DS London, U.K. (e-mail: bly@zepler.net).

Digital Object Identifier 10.1109/TVT.2006.889571

[1]A condensed version of this paper was presented at VTC'04 Fall, Los Angeles, CA.

[2]The diversity product or coding advantage was defined as the estimated gain over an uncoded system having the same diversity order as the coded system [6].

transmitted over the additive-white-Gaussian-noise (AWGN) channel, the authors of [14] proposed the employment of a density-evolution algorithm, which was also employed in [15] and [16] for the sake of constructing LDPC codes capable of operating at low E_b/N_0 values. Signal-to-noise-ratio (SNR)-based measures were used in [17] and [18] for studying the convergence of iterative decoders, while the authors of [19] investigated the convergence behavior of inner rate-one codes based on a combination of SNR measures and mutual information. In [20] and [21], ten Brink proposed the employment of the so-called extrinsic-information-transfer (EXIT) characteristics between a concatenated decoder's output and input for describing the flow of extrinsic information through the soft-in/soft-out constituent decoders. A tutorial introduction to EXIT charts can be found in [23]. Additionally, several algorithms predicting the decoding convergence of iterative decoding schemes were compared in [24].

Motivated by the performance improvements reported in [6] and [12], we propose a novel system that exploits the advantages of both iterative demapping and decoding. The STBC-SP demapper of [6] was further developed for the sake of accepting the *a priori* information passed to it from the channel decoder as extrinsic information. As a benefit of the proposed solution, it will be demonstrated in Section VI that the proposed turbo-detection-aided STBC-SP scheme is capable of providing E_b/N_0 gains of about 20.2 and 2.0 dB at a bit error rate (BER) of 10^{-5} over the equivalent-throughput uncoded STBC-SP scheme of [6] and over a turbo-detected quadrature phase shift keying (QPSK)-modulated system based on the STBC schemes of [2] and [3].

This paper is organised as follows. In Section II, a brief description of the orthogonal STBC design using SP modulation is presented, followed by a system overview in Section III. Section IV shows how the STBC-SP demapper is modified for exploiting the *a priori* knowledge provided by the channel decoder. Section V provides our EXIT chart analysis, while our simulation results and discussions are provided in Section VI. Finally, we conclude in Section VII.

II. Orthogonal Design With SP Modulation

This section describes the STBC-SP scheme proposed in [6], considering space-time systems employing two transmit antennas, where the space-time signal is given by [2]

$$\mathbf{G}_2(x_1, x_2) = \begin{bmatrix} x_1 & x_2 \\ -x_2^* & x_1^* \end{bmatrix} \tag{1}$$

and the rows and columns of (1) represent the temporal and spatial dimensions, corresponding to two consecutive time slots and two transmit antennas, respectively. According to Alamouti's design [2], for example, x_1 and x_2 represent conventional BPSK modulated symbols transmitted in the first and second time slots and no effort is made to jointly design a signal constellation for the various combinations of x_1 and x_2. For the sake of generalizing our treatment, let us assume that there are L legitimate space-time signals $\mathbf{G}_2(x_{l,1}, x_{l,2})$, $l = 0, 1, \ldots, L-1$, where L represents the number of SP modulated symbols. The transmitter, then, has to choose the modulated signal from these L legitimate symbols, which have to be transmitted over the two antennas in two consecutive time slots where the throughput of the system is given by $(\log_2 L)/2$ bits-per-channel use. In contrast to Alamouti's independent design of the two time slots' signals, our aim is to design $x_{l,1}$ and $x_{l,2}$ jointly, such that they have the best minimum Euclidean distance from all other $(L-1)$ legitimate transmitted space-time signals, since this minimizes the system's error probability. Let $(a_{l,1}, a_{l,2}, a_{l,3}, a_{l,4})$, $l = 0, 1, \ldots, L-1$ be phasor points from the 4-D real-valued Euclidean space $\mathbb{R}^4$, where each of the four elements $a_{l,1}, a_{l,2}, a_{l,3}$, and $a_{l,4}$ gives one coordinate of the two time-slots' complex-valued phasor points. Hence, $x_{l,1}$ and $x_{l,2}$ may be written as

$$\begin{aligned} \{x_{l,1}, x_{l,2}\} &= T(a_{l,1}, a_{l,2}, a_{l,3}, a_{l,4}) \\ &= \{a_{l,1} + j a_{l,2}, a_{l,3} + j a_{l,4}\}. \end{aligned} \tag{2}$$

In the 4-D real-valued Euclidean space $\mathbb{R}^4$, the lattice D_4 is defined as a SP having the best minimum Euclidean distance from all other $(L-1)$ legitimate constellation points in $\mathbb{R}^4$ [8]. More specifically, D_4 may be defined as a lattice that consists of all legitimate SP constellation points having integer coordinates $[a_1\ a_2\ a_3\ a_4]$ uniquely and unambiguously describing the legitimate combinations of the two time-slots' modulated symbols in Alamouti's scheme but subjected to the SP constraint of $a_1 + a_2 + a_3 + a_4 = k$, where k is an even integer. Assuming that $S = \{\mathbf{s}^l = [a_{l,1}\ a_{l,2}\ a_{l,3}\ a_{l,4}] \in \mathbb{R}^4 : 0 \le l \le L-1\}$ constitutes a set of L legitimate constellation points from the lattice D_4 having a total energy of $E \triangleq \sum_{l=0}^{L-1}(|a_{l,1}|^2 + |a_{l,2}|^2 + |a_{l,3}|^2 + |a_{l,4}|^2)$ and upon introducing the notation

$$\mathbf{C}_l = \sqrt{\frac{2L}{E}}\mathbf{G}_2(x_{l,1}, x_{l,2}), \qquad l = 0, 1, \ldots, L-1 \tag{3}$$

we have a set of space-time signals $\{\mathbf{C}_l : 0 \le l \le L-1\}$ whose diversity product is determined by the minimum Euclidean distance of the set of L legitimate constellation points in S.

III. System Overview

The schematic of the entire system is shown in Fig. 1, where the transmitted source bits are convolutionally encoded and then interleaved by a random-bit interleaver. A rate $R = 1/2$ recursive systematic convolutional code was employed. After channel interleaving, the SP mapper first maps B channel-coded bits $\mathbf{b} = b_{0,\ldots,B-1} \in \{0, 1\}$ to an SP modulated symbol $\mathbf{s} \in S$ such that we have $\mathbf{s} = \text{map}_{\text{sp}}(\mathbf{b})$, where $B = \log_2 L$. The STBC encoder then maps the SP modulated symbol $\mathbf{s}$ to a space-time signal $\mathbf{C}_l = \sqrt{2L/E}\ \mathbf{G}_2(x_{l,1}, x_{l,2})$, $0 \le l \le L-1$ using (1) and (2). Subsequently, each space-time signal is transmitted over $T = 2$ time slots using two transmit antennas.

In this treatise, we considered a correlated narrowband Rayleigh fading channel, based on the Jakes' fading model [25] and associated with a normalized Doppler frequency of $f_D = f_d T_s = 0.1$, where f_d is the Doppler frequency, and T_s is the symbol period. The complex fading envelope is assumed to be constant across the transmission period of a space-time coded

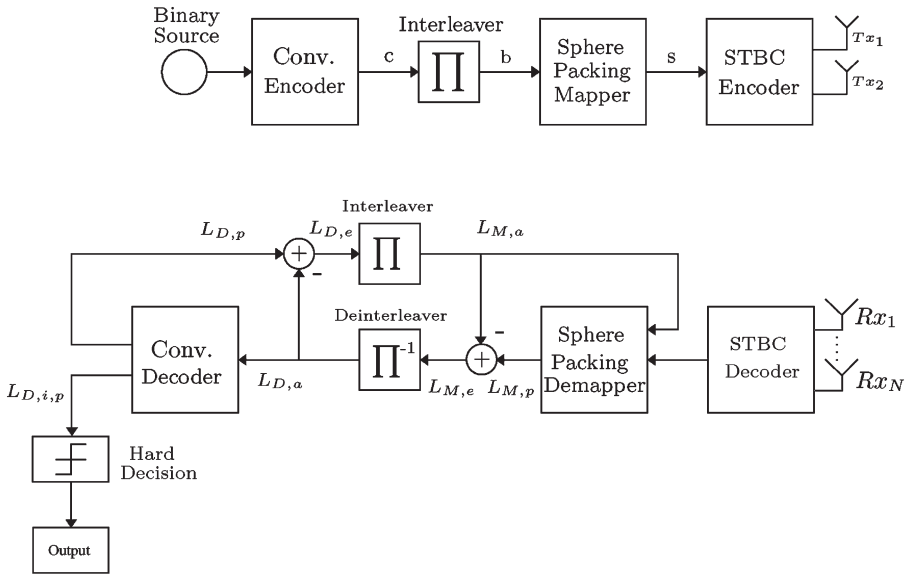

Fig. 1. Turbo-detection STBC-SP system.

symbol spanning $T = 2$ time slots. The complex AWGN of $n = n_I + jn_Q$ is also added to the received signal, where n_I and n_Q are two independent zero-mean Gaussian random variables having a variance of $\sigma_n^2 = \sigma_{n_I}^2 = \sigma_{n_Q}^2 = N_0/2$ per dimension, where $N_0/2$ represents the double-sided noise power spectral density expressed in watts per hertz.

As shown in Fig. 1, the received complex-valued symbols are demapped to their log-likelihood-ratio (LLR) representation for each of the B coded bits-per-STBC-SP symbol. The *a priori* LLR values of the demodulator are subtracted from the *a posteriori* LLR values for the sake of generating the extrinsic LLR values $L_{M,e}$, and then, the LLRs $L_{M,e}$ are deinterleaved by a soft-bit deinterleaver, as shown in Fig. 1. Next, the soft bits $L_{D,a}$ are passed to the convolutional decoder in order to compute the *a posteriori* LLR values $L_{D,p}$ provided by the max-log MAP algorithm [26] for all the channel-coded bits. During the last iteration, only the LLR values $L_{D,i,p}$ of the original uncoded-systematic-information bits are required, which are passed to a hard decision decoder in order to determine the estimated transmitted-source bits. The extrinsic information $L_{D,e}$ is generated by subtracting the *a priori* information from the *a posteriori* information according to $L_{D,p} - L_{D,a}$, which is then fed back to the STBC-SP demapper as the *a priori* information $L_{M,a}$ after appropriately reordering them using the interleaver of Fig. 1. The STBC-SP demapper exploits the *a priori* information for the sake of providing improved *a posteriori* LLR values, which are then passed to the channel decoder and, in turn, back to the STBC-SP demodulator for further iterations.

IV. Iterative Demapping

For the sake of simplicity, a system having a single-receive antenna is considered, although its extension to systems having more than one receive antenna is straightforward. Assuming perfect channel estimation, the complex-valued channel-output symbols received during two consecutive time slots are first diversity-combined in order to extract the estimates $\tilde{x}_1$ and $\tilde{x}_2$ of the most likely transmitted symbols $x_{l,1}$ and $x_{l,2}$ [2], [1, pp. 400–401], resulting in

$$\tilde{x}_1 = \left(|h_1|^2 + |h_2|^2\right) \cdot x_{l,1} + \acute{n}_1 \tag{4}$$

$$\tilde{x}_2 = \left(|h_1|^2 + |h_2|^2\right) \cdot x_{l,2} + \acute{n}_2 \tag{5}$$

where h_1 and h_2 represent the complex-valued channel coefficients corresponding to the first and second transmit antenna, respectively, and $\acute{n}_1$ as well as $\acute{n}_2$ are zero-mean complex Gaussian random variables with variance $\sigma_{\acute{n}}^2 = (|h_1|^2 + |h_2|^2) \cdot \sigma_n^2$. A received SP symbol $\mathbf{r}$ is then constructed from the estimates $\tilde{x}_1$ and $\tilde{x}_2$, using (2) as

$$\mathbf{r} = T^{-1}(\tilde{x}_1, \tilde{x}_2) \tag{6}$$

where $\mathbf{r} = \{[\tilde{a}_1\ \tilde{a_2}\ \tilde{a_3}\ \tilde{a_4}] \in \mathbb{R}^4\}$. The received SP symbol $\mathbf{r}$ can be written as

$$\mathbf{r} = h \cdot \sqrt{\frac{2L}{E}} \cdot \mathbf{s}^l + \mathbf{w} \tag{7}$$

where $h = (|h_1|^2 + |h_2|^2)$, $\mathbf{s}^l \in S$, $0 \le l \le L-1$, and $\mathbf{w}$ is a 4-D real-valued Gaussian random variable having a covariance matrix of $\sigma_w^2 \cdot \mathbf{I}_{N_D} = \sigma_{\acute{n}}^2 \cdot \mathbf{I}_{N_D} = h \cdot \sigma_n^2 \cdot \mathbf{I}_{N_D}$, where $N_D = 4$, since the symbol constellation S is 4-D. According to (7), the conditional PDF $p(\mathbf{r}|\mathbf{s}^l)$ is given by

$$\begin{aligned} p(\mathbf{r}|\mathbf{s}^l) &= \frac{1}{(2\pi\sigma_w^2)^{\frac{N_D}{2}}} e^{-\frac{1}{2\sigma_w^2}(\mathbf{r}-\alpha\cdot\mathbf{s}^l)(\mathbf{r}-\alpha\cdot\mathbf{s}^l)^{\mathrm{T}}} \\ &= \frac{1}{(2\pi\sigma_w^2)^{\frac{N_D}{2}}} e^{-\frac{1}{2\sigma_w^2}\left(\sum_{i=1}^{4}(\tilde{a}_i-\alpha\cdot a_{l,i})^2\right)} \end{aligned} \tag{8}$$

where we have $\alpha = h \cdot \sqrt{2L/E}$, and $(\cdot)^{\mathrm{T}}$ represents the transpose of a vector.

The SP symbol $\mathbf{r}$ carries B channel-coded bits $\mathbf{b} = b_{0,\ldots,B-1} \in \{0,1\}$. The LLR-value of bit k for $k = 0, \ldots, B-1$ can be written as [12]

$$L(b_k/\mathbf{r}) = L_a(b_k) + \ln \frac{\sum_{\mathbf{s}^l \in S_1^k} p(\mathbf{r}|\mathbf{s}^l) \cdot e^{\sum_{j=0, j\neq k}^{B-1} b_j L_a(b_j)}}{\sum_{\mathbf{s}^l \in S_0^k} p(\mathbf{r}|\mathbf{s}^l) \cdot e^{\sum_{j=0, j\neq k}^{B-1} b_j L_a(b_j)}} \tag{9}$$

where S_1^k and S_0^k are subsets of the symbol constellation S such that $S_1^k \triangleq \{\mathbf{s}^l \in S : b_k = 1\}$, and likewise, $S_0^k \triangleq \{\mathbf{s}^l \in S : b_k = 0\}$. In other words, S_i^k represents all symbols of the set S, where we have $b_k = i \in \{0,1\}$, $k = 0, \ldots, B-1$. Using (8), we can write (9) as

$$\begin{aligned} &L(b_k/\mathbf{r}) \\ &= L_a(b_k) \\ &\quad + \ln \frac{\sum_{\mathbf{s}^l \in S_1^k} e^{\left[-\frac{1}{2\sigma_w^2}(\mathbf{r}-\alpha\cdot\mathbf{s}^l)(\mathbf{r}-\alpha\cdot\mathbf{s}^l)^{\mathrm{T}} + \sum_{j=0, j\neq k}^{B-1} b_j L_a(b_j)\right]}}{\sum_{\mathbf{s}^l \in S_0^k} e^{\left[-\frac{1}{2\sigma_w^2}(\mathbf{r}-\alpha\cdot\mathbf{s}^l)(\mathbf{r}-\alpha\cdot\mathbf{s}^l)^{\mathrm{T}} + \sum_{j=0, j\neq k}^{B-1} b_j L_a(b_j)\right]}} \\ &= L_{M,a} + L_{M,e}. \end{aligned} \tag{10}$$

Finally, the max-log approximation of (10) is as follows:

$$\begin{aligned} &L(b_k/\mathbf{r}) \\ &= L_a(b_k) \\ &\quad + \max_{\mathbf{s}^l \in S_1^k} \left[-\frac{1}{2\sigma_w^2}(\mathbf{r}-\alpha\cdot\mathbf{s}^l)(\mathbf{r}-\alpha\cdot\mathbf{s}^l)^{\mathrm{T}} + \sum_{j=0, j\neq k}^{B-1} b_j L_a(b_j) \right] \\ &\quad - \max_{\mathbf{s}^l \in S_0^k} \left[-\frac{1}{2\sigma_w^2}(\mathbf{r}-\alpha\cdot\mathbf{s}^l)(\mathbf{r}-\alpha\cdot\mathbf{s}^l)^{\mathrm{T}} + \sum_{j=0, j\neq k}^{B-1} b_j L_a(b_j) \right]. \end{aligned} \tag{11}$$

V. EXIT-Chart Analysis

The main objective of employing EXIT charts proposed by ten Brink [20], [21] is to predict the convergence behavior of the iterative decoder by examining the evolution of the input/output mutual-information exchange between the inner and outer decoders in consecutive iterations. The application of EXIT charts is based on two assumptions, namely, that upon assuming large interleaver lengths, 1) the *a priori* LLR values are fairly uncorrelated, and 2) the probability density function of the *a priori* LLR values is Gaussian.

A. Transfer Characteristics of the Demapper

As shown in Fig. 1, the inputs of the SP demapper are the noise-contaminated channel observations and the *a priori* information $L_{M,a}$ generated by the outer channel decoder. The demapper outputs the *a posteriori* information $L_{M,p}$, subtracts the *a priori* and, hence, produces the extrinsic information $L_{M,e}$, as shown in Section IV. Based on the aforementioned two assumptions, the *a priori* input $L_{M,a}$ can be modeled by applying an independent zero-mean Gaussian random variable n_A having a variance of σ_A^2. In conjunction with the outer channel coded and interleaved bits $b \in \{0,1\}$ of Fig. 1 or equivalently $x \in \{-1,+1\}$, the *a priori* input $L_{M,a}$ can be written as [20]

$$L_{M,a} = \mu_A \cdot x + n_A \tag{12}$$

where $\mu_A = \sigma_A^2/2$, since $L_{M,a}$ is an LLR-value obeying the Gaussian distribution [27]. The mutual information of $I_{A_M} = I(X; L_{M,a})$, $0 \leq I_{A_M} \leq 1$ between the outer coded and interleaved bits x and the LLR values $L_{M,a}$ is used to quantify the information content of the *a priori* knowledge [28]

$$\begin{aligned} I_{A_M} = \frac{1}{2} \cdot \sum_{x=-1,+1} \int_{-\infty}^{+\infty} & p_A(\zeta|X=x) \\ & \times \log_2 \frac{2 \cdot p_A(\zeta|X=x)}{p_A(\zeta|X=-1) + p_A(\zeta|X=+1)} d\zeta. \end{aligned} \tag{13}$$

It was shown in [22] that the mutual information between the equiprobable bits x and their respective LLRs L for symmetric and consistent[3] L-values always simplifies to

$$\begin{aligned} I(X;L) &= 1 - \int_{-\infty}^{+\infty} p(L|X=+1) \cdot \log_2[1+e^{-L}] dL \\ I(X;L) &= 1 - E_{X=+1}\left\{\log_2[1+e^{-L}]\right\}. \end{aligned} \tag{14}$$

In order to quantify the information content of the extrinsic LLR values $L_{M,e}$ at the output of the demapper, the mutual information $I_{E_M} = I(X; L_{M,e})$ can be used, which could be computed as in (13) using the PDF p_E of the extrinsic output, which requires the determination of the distribution p_E by means of Monte Carlo simulations. However, according to [22], by invoking the ergodicity theorem in (14), namely, by replacing the expected value by the time average, the mutual information can be estimated using a sufficiently large number of samples even for non-Gaussian or unknown distributions, which may be expressed as [22]

$$\begin{aligned} I_{E_M} &= I(X; L_{M,e}) = 1 - E_{X=+1}\left\{\log_2[1+e^{-L_{M,e}}]\right\} \\ &\approx 1 - \frac{1}{N}\sum_{n=1}^{N} \log_2[1+e^{-x(n)\cdot L_{M,e}(n)}]. \end{aligned} \tag{15}$$

Considering I_{E_M} as a function of both I_{A_M} and the E_b/N_0 value encountered, the demapper's EXIT characteristic is defined as [20], [21]

$$I_{E_M} = T_M(I_{A_M}, E_b/N_0). \tag{16}$$

[3]The LLR values are symmetric if their PDF is symmetric i.e., when we have $p(-\zeta|X=+1) = p(\zeta|X=-1)$. Additionally, all LLR values having symmetric distributions satisfy the consistency condition [22]: $p(-\zeta|X=x) = e^{-x\zeta}p(\zeta|X=x)$.

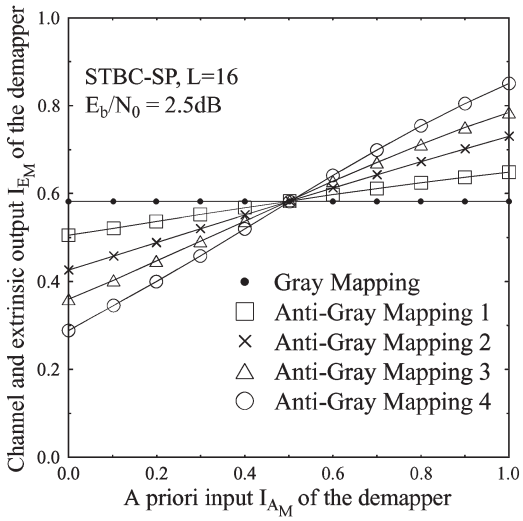

Fig. 2. SP demapper EXIT characteristics for different bits-to-SP symbol-mapping schemes at $E_b/N_0 = 2.5$ dB for $L = 16$.

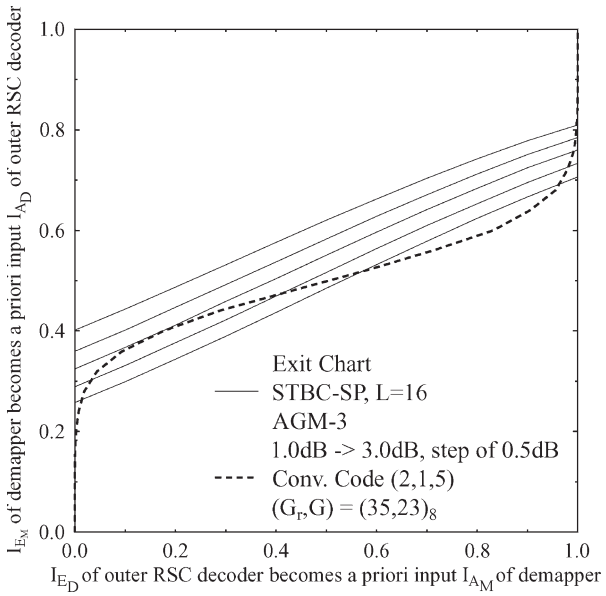

Fig. 3. EXIT chart of a turbo-detected RSC channel-coded STBC-SP scheme employing AGM-3 of Fig. 2 in combination with the outer RSC code and system parameters outlined in Table I.

Fig. 2 shows the EXIT characteristics of the SP demapper in conjunction with $L = 16$ and different mapping schemes between the interleaver's output and the STBC encoder. As expected, Gray mapping (GM) does not provide any iteration gain upon increasing the mutual information at the input of the demapper. However, using a variety of different anti-Gray mapping (AGM) schemes [12] results in different EXIT characteristics, as illustrated by the different slopes shown in Fig. 2. The four different AGM mapping schemes shown in Fig. 2 are specifically selected from all the possible mapping schemes for $L = 16$ in order to demonstrate the different EXIT characteristics associated with different bit-to-symbol mapping schemes. There are a total of 16! different mapping schemes. Both the GM as well as the various AGM mapping schemes considered in this paper are detailed in Appendix.

B. Transfer Characteristics of the Outer Decoder

The extrinsic transfer characteristic of the outer channel decoder describes the relationship between the outer channel coded input $L_{D,a}$ and the outer channel decoded extrinsic output $L_{D,e}$. The input of the outer channel decoder is constituted by the *a priori* input $L_{D,a}$ provided by the SP demapper. Therefore, the EXIT characteristic of the outer channel decoder is independent of the E_b/N_0-value and, hence, may be written as

$$I_{E_D} = T_D(I_{A_D}) \tag{17}$$

where $I_{A_D} = I(C; L_{D,a})$, $0 \le I_{A_D} \le 1$ is the mutual information between the outer channel coded bits c and the LLR values $L_{D,a}$. Similarly, $I_{E_D} = I(C; L_{D,e})$, $0 \le I_{E_D} \le 1$ is the mutual information between the outer channel coded bits c and the LLR values $L_{D,e}$.

C. EXIT Chart

The exchange of extrinsic information in the system schematic of Fig. 1 is visualized by plotting the EXIT characteristics of the SP demapper and the outer RSC decoder in a joint diagram. This diagram is known as the EXIT chart [20], [21].

TABLE I
SYSTEM PARAMETERS

Modulation	Sphere Packing with $L = 16$
No. of Transmitters	2
No. of Receivers	1
Channel	Correlated Rayleigh Fading
Normalized Doppler frequency	0.1
Outer channel code	RSC, $(2, 1, 5)$ $(G_r, G) = (35, 23)_8$
System throughput	1 bit/symbol

The outer RSC decoder's extrinsic output I_{E_D} becomes the SP demapper's *a priori* input I_{A_M}, which is represented on the x-axis. Similarly, on the y-axis, the SP demapper's extrinsic output I_{E_M} becomes the outer RSC decoder's *a priori* input I_{A_D}.

Fig. 3 shows the EXIT chart of a turbo-detection-aided channel-coded STBC-SP scheme employing the AGM-3 of Fig. 2, in conjunction with the outer RSC code and the system parameters outlined in Table I. Ideally, in order for the exchange of extrinsic information between the SP demapper and the outer RSC decoder to converge at a specific E_b/N_0 value, the extrinsic-transfer curve of the SP demapper recorded at the E_b/N_0 value of interest and the extrinsic-transfer-characteristic curve of the outer RSC decoder should only intersect at a point infinitesimally close to the $I_{E_D} = 1.0$ line. If this condition is satisfied, then a so-called convergence tunnel [20], [21] appears in the EXIT chart. The narrower the tunnel, the more iterations are required for reaching the intersection point. Observe in Fig. 3 that a convergence tunnel exists at $E_b/N_0 = 2.5$ dB. This implies that according to the predictions of the EXIT chart shown in Fig. 3, the iterative decoding process is expected to converge, and hence, a low BER may be attained at $E_b/N_0 = 2.5$ dB. The validity of this prediction is, however, dependent on how accurately the two EXIT-chart assumptions outlined

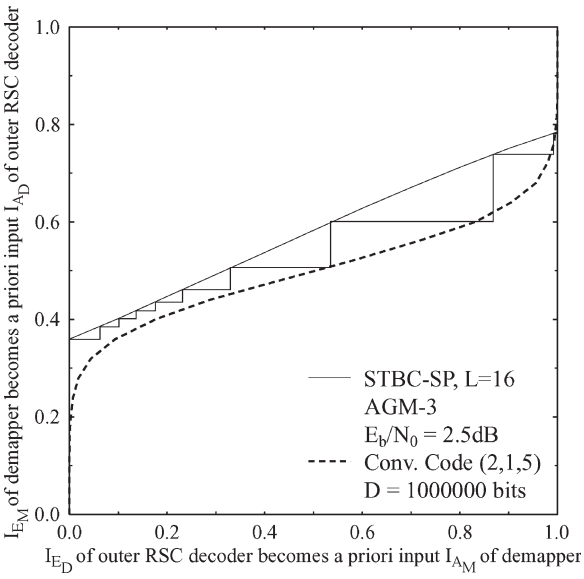

Fig. 4. Decoding trajectory of turbo-detected RSC channel-coded STBC-SP scheme employing AGM-3 in combination with the outer RSC code and system parameters outlined in Table I and operating at $E_b/N_0 = 2.5$ dB with an interleaver depth of $D = 10^6$ bits after ten external joint iterations.

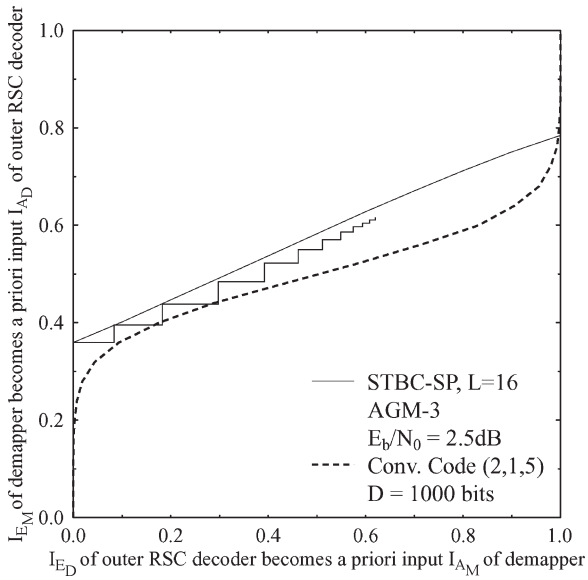

Fig. 5. Decoding trajectory of turbo-detected RSC channel-coded STBC-SP scheme employing AGM-3 in combination with the outer RSC code and system parameters outlined in Table I and operating at $E_b/N_0 = 2.5$ dB with an interleaver depth of $D = 10^3$ bits after ten external joint iterations.

at the beginning of Section V are satisfied. These EXIT-chart-based convergence predictions are usually verified by the actual iterative decoding trajectory, as will be discussed in Section VI.

VI. Results and Discussion

Without loss of generality, we considered a SP modulation scheme associated with $L = 16$ using two transmit and a single receiver antenna in order to demonstrate the performance improvements achieved by the proposed system. All simulation parameters are listed in Table I.

Since the space-time signal, which is constructed from an orthogonal design using the SP scheme of (3), is multiplied by a factor that is inversely proportional to $\sqrt{E}$, namely, by $\sqrt{2L/E}$, it is desirable to choose a specific subset of $L = 16$ points from the entire set of legitimate constellation points hosted by D_4, which results in the minimum total energy. It was shown in [8] that there is a total of 24 legitimate symbols[4] hosted by D_4 having an identical minimum energy of $E = 2$. We used a computer search for determining the optimum choice of the $L = 16$ points out of the possible 24 points, which possess the highest minimum Euclidean distance, hence minimizing the error probability.

Fig. 4 illustrates the actual decoding trajectory of the turbo-detected RSC channel-coded STBC-SP scheme of Fig. 3 at $E_b/N_0 = 2.5$ dB and using an interleaver depth of $D = 10^6$ bits. The zigzag-path shown in Fig. 4 represents the actual EXIT between the SP demapper and the outer RSC channel decoder. Since a long interleaver is employed, the assumptions outlined at the beginning of Section V are justified, and hence, the EXIT-chart-based convergence prediction has been attained.

[4]In simple terms, the sphere centered at (0, 0, 0, 0) has 24 spheres around it, centered at the points $(+/-1, +/-1, 0, 0)$, where any choice of signs and any ordering of the coordinates is legitimate [7, p. 9].

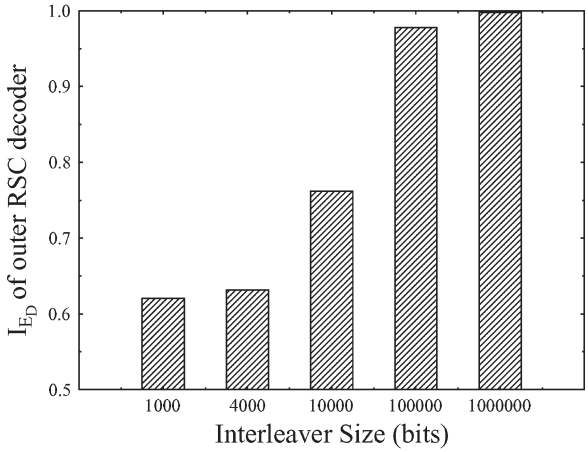

Fig. 6. Achievable extrinsic information of turbo-detected RSC channel-coded STBC-SP scheme employing AGM-3 in combination with the outer RSC code and system parameters outlined in Table I and operating at $E_b/N_0 = 2.5$ dB with different interleaver depths after ten external-joint iterations.

However, the decoding trajectory shown in Fig. 5 is different from the EXIT-chart prediction, because a shorter interleaver length is used. The achievable I_{E_D} associated with employing different interleaver lengths is demonstrated in Fig. 6. The BER curves of the schemes characterized in Fig. 6 are shown in Fig. 7 when using ten external joint iterations, demonstrating the achievable BER difference at $E_b/N_0 = 2.5$ dB when increasing the interleaver length to $D = 10^6$ bits. Additionally, observe the turbo cliff taking shape at $E_b/N_0 = 2.5$ dB upon increasing the interleaver length.

Fig. 8 compares the performance of the proposed convolutional-coded STBC-SP scheme employing AGM-3 and GM against that of an identical-throughput 1-bit-per-symbol (1BPS) uncoded STBC-SP scheme and a conventional orthogonal STBC design, as well as against an RSC-coded QPSK modulated STBC scheme when communicating over a

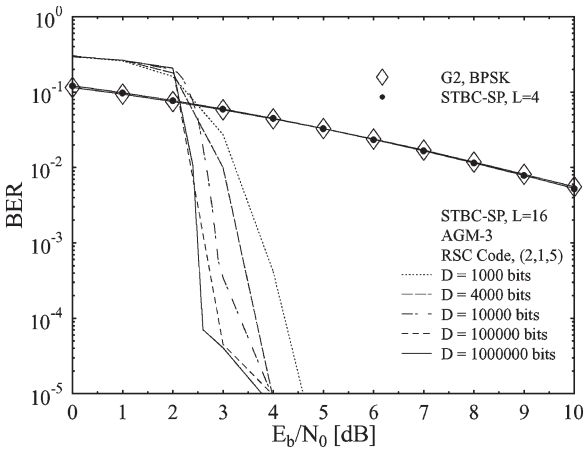

Fig. 7. Performance comparison of AGM-3-based RSC-coded STBC-SP schemes in conjunction with $L = 16$ against an identical-throughput 1BPS uncoded STBC-SP scheme using $L = 4$ and against Alamouti's conventional $\mathbf{G}_2$-BPSK scheme, after ten external-joint iterations and using different interleaver depths. The remaining system parameters are listed in Table I.

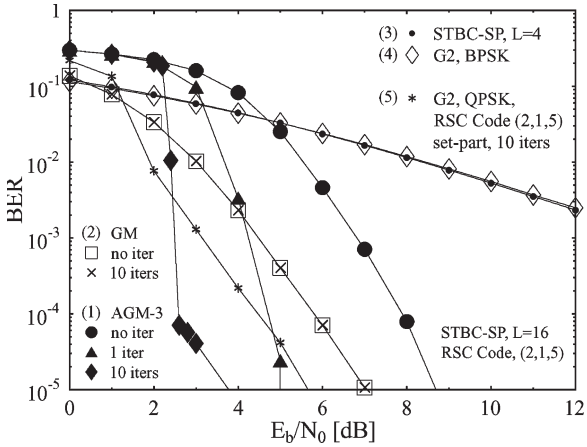

Fig. 8. Performance comparison of AGM-3$^{(1)}$ and GM$^{(2)}$-based RSC-coded STBC-SP schemes in conjunction with $L = 16$ against an identical-throughput 1BPS uncoded STBC-SP scheme$^{(3)}$ using $L = 4$ and against Alamouti's conventional $\mathbf{G}_2$-BPSK scheme$^{(4)}$, as well as against an RSC-coded QPSK modulated STBC scheme$^{(5)}$ when employing the system parameters outlined in Table I and using an interleaver depth of $D = 10^6$ bits.

correlated Rayleigh fading channel. An interleaver depth of $D = 10^6$ bits was employed, and a normalized Doppler frequency of $f_D = 0.1$ was used. The QPSK modulated STBC system employs a set-partitioning mapping scheme reminiscent of Trellis-coded modulation [29]. Observe in Fig. 8, by comparing the two GM STBC-SP curves, that no BER improvement was obtained when ten turbo-detection iterations were employed in conjunction with GM, which was reported also in [12] and evident from the flat curve of the GM in Fig. 2. By contrast, AGM-3 achieved a useful performance improvement in conjunction with iterative demapping and decoding. Explicitly, Fig. 8 demonstrates that a coding advantage of about 20.2 dB was achieved at a BER of 10^{-5} after ten iterations by the convolutional-coded AGM-3 STBC-SP system over both the uncoded STBC-SP [6] and the conventional orthogonal STBC design-based [2], [3] schemes for transmission over the correlated Rayleigh fading channel considered. Additionally, coding advantages of approximately 3.2 and 2.0 dB were attained over the 1BPS-throughput RSC-coded GM STBC-SP and the RSC-coded QPSK modulated STBC schemes, respectively. The employment of SP of size $L = 16$, as opposed to QPSK, would double the number of metrics to be computed in the demapper.

TABLE II
BIT MAPPINGS FOR THE GM AND THE FOUR DIFFERENT AGM SCHEMES INTRODUCED IN SECTION V FOR STBC-SP SIGNALS OF SIZE $L = 16$

Points from D_4				Integer Index				
a_1	a_2	a_3	a_4	GM	AGM-1	AGM-2	AGM-3	AGM-4
−1	−1	0	0	0	15	12	15	0
0	−1	−1	0	1	1	1	11	11
0	−1	+1	0	2	2	10	7	7
+1	−1	0	0	3	3	5	12	12
−1	0	0	+1	4	4	0	14	14
0	0	−1	+1	5	5	4	5	5
0	0	+1	+1	6	6	8	9	9
+1	0	0	+1	7	7	14	2	2
−1	0	0	−1	8	8	9	13	13
0	0	−1	−1	9	9	15	6	6
0	0	+1	−1	10	10	2	10	10
+1	0	0	−1	11	11	7	1	1
−1	+1	0	0	12	12	13	3	3
0	+1	−1	0	13	13	3	8	8
0	+1	+1	0	14	14	11	4	4
+1	+1	0	0	15	0	6	0	15

VII. CONCLUSION

In this paper, we proposed a novel system that exploits the advantages of both iterative demapping and turbo detection [12], as well as those of the STBC-SP scheme of [6]. Our investigations demonstrated that significant performance improvements may be achieved when the AGM STBC-SP scheme is combined with outer channel decoding and iterative demapping, as compared to the GM-based systems. Subsequently, EXIT charts were used to search for the optimum bit-to-symbol mapping schemes that converge at the lowest possible E_b/N_0 values. Several STBC-SP mapping schemes covering a wide range of extrinsic transfer characteristics were investigated. When using an appropriate bit-to-symbol mapping scheme and ten turbo-detection iterations, an E_b/N_0 gain of about 20.2 dB was obtained by the convolutional-coded STBC-SP scheme over the identical-throughput 1BPS uncoded STBC-SP benchmarker scheme of [6].

APPENDIX
GM AND AGM SCHEMES FOR SP MODULATION OF SIZE $L = 16$

In this Appendix, GM and the four different AGM schemes introduced in Section V for STBC-SP signals of size $L = 16$ are described in detail. More specifically, for all mapping schemes, constellation points of the lattice D_4 are given for each integer index $l = 0, 1, \ldots, 15$. Observe that all mapping schemes use the same 16 constellation points from the entire set of 24 points, which were selected by finding the highest minimum Euclidean distance, as described in Section VI. The normalization factor of these constellation points is $\sqrt{2L/E} = 1$, where E is as defined in Section II. The constellation points corresponding to each mapping scheme are given in Table II.

ACKNOWLEDGMENT

The authors would like to thank the anonymous reviewers for their valuable comments that led to a substantially improved manuscript.

REFERENCES

[1] L. Hanzo, T. H. Liew, and B. L. Yeap, *Turbo Coding, Turbo Equalisation and Space-Time Coding: For Transmission over Fading Channels*. Chichester, U.K.: Wiley, 2002.

[2] S. Alamouti, "A simple transmit diversity technique for wireless communications," *IEEE J. Sel. Areas Commun.*, vol. 16, no. 8, pp. 1451–1458, Oct. 1998.

[3] V. Tarokh, H. Jafarkhani, and A. Calderbank, "Space-time block codes from orthogonal designs," *IEEE Trans. Inf. Theory*, vol. 45, no. 5, pp. 1456–1467, Jul. 1999.

[4] ——, "Space-time block coding for wireless communications: Performance results," *IEEE J. Sel. Areas Commun.*, vol. 17, no. 3, pp. 451–460, Mar. 1999.

[5] B. M. Hochwald, G. Caire, B. Hassibi, and E. T. L. Marzetta, "Special issue on space-time transmission, reception, coding and signal processing," *IEEE Trans. Inf. Theory*, vol. 49, no. 10, pp. 2329–2806, Oct. 2003.

[6] W. Su, Z. Safar, and K. J. R. Liu, "Space-time signal design for time-correlated Rayleigh fading channels," in *Proc. IEEE Int. Conf. Commun.*, Anchorage, AK, May 2003, vol. 5, pp. 3175–3179.

[7] W. Su and X. G. Xia, "On space-time block codes from complex orthogonal designs," *Wirel. Pers. Commun.*, vol. 25, no. 1, pp. 1–26, Apr. 2003.

[8] J. H. Conway and N. J. Sloane, *Sphere Packings, Lattices and Groups*. New York: Springer-Verlag, 1999.

[9] S. L. Goff, A. Glavieux, and C. Berrou, "Turbo-codes and high spectral efficiency modulation," in *Proc. Int. Conf. Commun.*, New Orleans, LA, May 1994, pp. 645–649.

[10] T. Mittelholzer, X. Lin, and J. Massey, "Multilevel turbo coding for M-ary quadrature and amplitude modulation," in *Proc. Int. Symp. Turbo Codes and Related Topics*, Brest, France, Sep. 1997, pp. 127–134.

[11] P. Robertson, "An overview of bandwidth efficient turbo coding schemes," in *Proc. Int. Symp. Turbo Codes and Related Topics*, Brest, France, Sep. 1997, pp. 103–110.

[12] S. ten Brink, J. Speidel, and R.-H. Yan, "Iterative demappping and decoding for multilevel modulation," in *Proc. IEEE Global Telecommun. Conf.*, Sydney, Australia, Nov. 8–12, 1998, vol. 1, pp. 579–584.

[13] A. Sezgin, D. Wuebben, and V. Kuehn, "Analysis of mapping strategies for turbo-coded space-time block codes," in *Proc. IEEE Inf. Theory Workshop*, Mar. 2003, pp. 103–106.

[14] T. J. Richardson and R. Urbanke, "The capacity of low-density parity-check codes under message-passing decoding," *IEEE Trans. Inf. Theory*, vol. 47, no. 2, pp. 599–618, Feb. 2001.

[15] T. J. Richardson, A. Shokrollahi, and R. Urbanke, "Design of capacity-approaching low-density parity-check codes," *IEEE Trans. Inf. Theory*, vol. 47, no. 2, pp. 619–637, Feb. 2001.

[16] S. Y. Chung, G. D. Forney, T. J. Richardson, and R. Urbanke, "On the design of low-density parity-check codes within 0.0045 dB of the Shannon limit," *IEEE Commun. Lett.*, vol. 5, no. 2, pp. 58–60, Feb. 2001.

[17] H. E. Gamal and A. R. Hammons, "Analyzing the turbo decoder using the Gaussian approximation," *IEEE J. Sel. Areas Commun.*, vol. 47, no. 2, pp. 671–686, Feb. 2001.

[18] D. Divsalar, S. Dolinar, and F. Pollara, "Low complexity turbo-like codes," in *Proc. 2nd Int. Symp. Turbo Codes and Related Topics*, Brest, France, Sep. 2000, pp. 73–80.

[19] M. Peleg, I. Sason, S. Shamai, and A. Elia, "On interleaved differentially encoded convolutional codes," *IEEE Trans. Inf. Theory*, vol. 45, no. 7, pp. 2572–2582, Nov. 1999.

[20] S. ten Brink, "Designing iterative decoding schemes with the extrinsic information transfer chart," *AEÜ, Int. J. Electron. Commun.*, vol. 54, no. 6, pp. 389–398, Nov. 2000.

[21] ——, "Convergence behaviour of iteratively decoded parallel concatenated codes," *IEEE Trans. Commun.*, vol. 49, no. 10, pp. 1727–1737, Oct. 2001.

[22] M. Tuechler and J. Hagenauer, "EXIT charts of irregular codes," in *Proc. 36th Annu. CISS*, Princeton, NJ, Mar. 2002, pp. 748–753.

[23] J. Hagenauer, "The EXIT chart—Introduction to extrinsic information transfer in iterative processing," in *Proc. Eur. Signal Process. Conf.*, Vienna, Austria, Sep. 2004, pp. 1541–1548.

[24] M. Tuechler, S. ten Brink, and J. Hagenauer, "Measures for tracing convergence of iterative decoding algorithms," in *Proc. 4th Int. ITG Conf. Source and Channel Coding*, Berlin, Germany, Jan. 2002, pp. 53–60.

[25] W. C. Jakes, *Microwave Mobile Communications*. New York: Wiley, 1974.

[26] P. Robertson, E. Villebrun, and P. Hoeher, "A comparison of optimal and sub-optimal MAP decoding algorithms operating in the log domain," in *Proc. Int. Conf. Commun.*, Seattle, WA, Jun. 1995, pp. 1009–1013.

[27] J. Hagenauer, E. Offer, and L. Papke, "Iterative decoding of binary block and convolutional codes," *IEEE Trans. Inf. Theory*, vol. 42, no. 2, pp. 429–445, Mar. 1996.

[28] T. M. Cover and J. A. Thomas, *Elements of Information Theory*. New York: Wiley, 1991.

[29] G. Ungerboeck, "Channel coding with multilevel/phase signals," *IEEE Trans. Inf. Theory*, vol. IT-28, no. 1, pp. 55–67, Jan. 1982.

Osamah Rashed Alamri received the B.S. degree (with first-class honors) in electrical engineering from King Fahd University of Petroleum and Minerals, Dhahran, Saudi Arabia, in 1997 and the M.S. degree in electrical engineering from Stanford University, Stanford, CA, in 2002. Since October 2002, he has been working toward the Ph.D. degree at the Communications Group, School of Electronics and Computer Science, University of Southampton, Southampton, U.K.

His research interests include sphere-packing modulation, space-time coding, turbo coding and detection, adaptive receivers, and multiple-input–multiple-output (MIMO) systems.

Bee Leong Yeap received the degree (with first-class honors) in electronics engineering and the Ph.D. degree from the University of Southampton, Southampton, U.K., in 1996 and 2000, respectively.

He continued his research as a Postdoctoral Research Fellow with Southampton until 2004, when he joined Radioscape: a London, U.K. based consultancy company. His research interests include turbo coding, turbo equalization, adaptive modulation, and space-time coding. More recently, he embarked on conducting research into the implementation of digital radio receivers.

Lajos Hanzo (M'91–SM'92–F'04) received the Master's degree in electronics and the Ph.D. degree in 1976 and 1983, respectively. He received the Doctor of Sciences (D.Sc.) degree from the University Southampton, Southampton, U.K., in 2004.

During his 30-year career in telecommunications, he has held various research and academic posts in Hungary, Germany, and the U.K. Since 1986, he has been with the Department of Electronics and Computer Science, University of Southampton, where he holds the Chair in telecommunications. He has coauthored 15 John Wiley/IEEE Press books totaling about 10 000 pages on mobile-radio communications, published about 700 research papers, organized and chaired conference sessions, presented overview lectures, and has been awarded a number of distinctions. He is a Nonexecutive Director of the Virtual Centre of Excellence, U.K., and an enthusiastic supporter of industrial–academic liaison. He also offers a range of industrial research overview courses.

Dr. Hanzo is an IEEE Distinguished Lecturer of both the Communications Society and the Vehicular Technology Society. He is a Fellow of the Royal Academy of Engineering (FREng) and of the IEE. He is a Governor of the IEEE Vehicular Technology Society and an Editor of the PROCEEDINGS OF THE IEEE.